Int. J. Heat Mass Transfer. Vol. 23, pp. 873–880
Pergamon Press Ltd. 1980. Printed in Great Britain

FULLY DEVELOPED LAMINAR FLOW AND HEAT TRANSFER IN CURVED TUBES

Z. ZAPRYANOV, CH. CHRISTOV and E. TOSHEV
Bulgarian Academy of Sciences, Institute of Mechanics and Biomechanics,
P.O. Box 373, Sofia 1000, Bulgaria

(*Received* 6 *December* 1978 *and in revised form* 18 *December* 1979)

Abstract—This paper deals with the extension of the method of fractional steps to hydrodynamic and thermal problems for fully developed steady flow of viscous incompressible fluid in a curved circular tube. This numerical method yields good solutions from low to reasonably high Dean and Prandtl numbers. Typical examples for axial velocity profiles and temperature profiles, streamlines and velocity profiles for secondary flow and isotherms are given. Comparison of the numerically computed velocity and temperature profiles were made with experimental data and some theoretical solutions.

NOMENCLATURE

u', v', w', velocity components in r, φ, θ directions respectively;
u, v, w, dimensionless components in r, φ, θ directions respectively;
T, local temperature;
T_w, wall temperature;
H, dimensionless temperature;
W_m, average velocity in direction θ;
a, radius of tube;
L, radius of curvature of the tube axis;
r, dimensionless radial coordinate;
Re, Reynolds number;
Pr, Prandtl number;
D, Dean number;
M, number of grid points of r-direction;
N, number of grid points of φ-direction;
r', radial coordinate in the tube cross section;
Nu, local Nusselt number;
$\bar{N}u$, peripherally averaged Nusselt number;
$\bar{N}u_0$, peripherally averaged Nusselt number for straight tube;
G_T, axial-temperature gradient;
t, time;
h, dimensionless grid spacing $1/(M-1)$;
l, dimensionless grid spacing $\pi/(N-1)$.

Greek symbols

ν, kinematic viscosity;
φ, angular coordinate in the tube cross section;
θ, angular coordinate normal to the tube cross section;
Ψ, stream function of the secondary flow;
ζ, vorticity in the cross section;
t_I, fictitious time.

Subscripts

i, j, space subscripts of grid point in r and φ directions;
m, flow-averaged mean value;
0, value for straight tube;
w, value at the wall.

Superscripts

p, pth iteration in the fictitious time;
n, nth time stage;
$-$, average value.

1. INTRODUCTION

INTEREST in the problem of heat transfer in fully-developed tube flows dates back over a hundred years. The forced convection problems in curved tubes are frequently encountered in various heat exchanges, cooling or heating systems, chemical reactors, heat engines and other apparatus, equipment and devices.

It is well known that the mode of fluid in a curved tube is characterized by a secondary flow field, which is superimposed upon the axial-velocity flow field. The nature of the viscous flow in a curved tube, as compared with simple straight-tube parabolic flow, causes relatively high average heat- and mass-transfer rates per unit axial pressure drop, especially for fluid with a high Prandtl number and high Schmidt number.

Of fundamental interest to the development of a complete understanding of viscous-flow phenomena in toroidal tubes is the nature of the velocity and temperature distributions in the fully-developed flow region. The first theoretical study of the fully developed steady flow in a curved tube with circular sections was made by Dean [1] in 1927. He pointed out that the dynamic similarity of such flow depends on a non-dimensional parameter $K = [(2a/L)(aW_m/\nu)^2]$ where W_m is the mean velocity along the pipe, ν the kinematic viscosity and a the radius of the pipe, which is bent in a circle with a radius L. Physically this parameter can be considered as the ratio of the centrifugal force induced by circular motion of the fluid to the viscous force. Dean's analysis of the toroidal flow was restricted to small values of K.

Barua [2] considered fully developed motion for

large K and obtained an approximation solution by a Karman–Pohlhausen momentum integral method. McConalogue and Srivastava [3] extended Dean's work and adopted a parameter $D = [4Re(2a/L)^{1/2}]$. Their numerical solutions were given over the range $D = 96$ to $D = 605.72$, the value corresponding to the upper limit $K = 576$ of Dean's work.

Truesdell and Adler [4] have obtained results up to $D = 3578$. Greenspan [5] and Collins and Dennis [6] have centered their interest on the following range of $D: 0 \leq D \leq 5000$. There are some discrepancies however, between previous numerical results. For example, Greenspan's calculations do not coincide with those of McConalogue and Srivastava. Greenspan used a finite difference method based on the so-called forward and backward difference scheme, while Collins and Dennis have used the difference correction method of Fox. The solution procedure requires to use the results from the previous value of D as an initial assumption. They have used the increment $\Delta D = 20$ from $D = 1000$ to $D = 2000$ and increments $\Delta D = 10$ for higher values of D. The computational procedure was found to converge satisfactorily only for solutions in the range $D = 96$–1000, but for the range $D = 2000$–5000 it was necessary to use a smoothing process for the corrections.

Recently, Zapryanov and Christov [7] have obtained a numerical solution of the same problem by the method of fractional steps. In contrast to the Collins and Dennis' work in our calculations the increments are $\Delta D \geq 500$.

Another approach, also including heat transfer in the curved tube has been given by Patankar *et al.* [8]. On the basis of the marching technique they have obtained fully-developed profiles independent of the axial direction for a wide range of values D.

Mori and Nakayama [9] obtained the first theoretical heat-transfer solutions by boundary-layer methods for the constant wall-temperature boundary conditions. It is shown by Dravid *et al.* [10] that Mori and Nakayama's Prandtl number dependence is inaccurate. Austin's solution [11] for fully developed velocity profiles was used by Kalb and Seader [12] in the study of the heat-transfer problem. The thermal-energy equation was solved numerically by use of a point successive-overrelaxation method. Solutions have been given for Prandtl number Pr varied from 0.005 to 1600.

The purpose of this paper is to present flow and heat transfer results obtained by a method of fractional steps for steady fully developed laminar flow in a curved circular tube under the thermal boundary conditions of constant wall temperature. Results are presented for the range 10–7000 of parameter D and for a Prandtl number varied from 0.005 to 2000.

2. FORMULATION OF THE PROBLEM

The present paper concerns a steady hydrodynamically and thermally fully-developed laminar flow, of incompressible viscous fluid in a curved circular tube

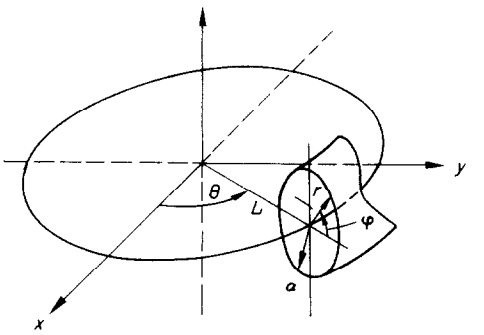

FIG. 1. System of toroidal coordinates for a curved circular tube.

under the thermal boundary condition of a uniform wall temperature. Figure 1 shows a system of toroidal coordinates (r, φ, θ) concerning the motion of the fluid through the pipe. The distance down the tube is measured by $L\theta$, where θ is the angular coordinate normal to the tube cross section. A point P in the cross section is located by the polar coordinates r and φ. The radius of the curvature of the coiled tube is denoted by L. Let (u, v, w) denote the velocity components in the (r, φ, θ) directions respectively.

We assume that the radius of curvature of the tube axis is large in comparison to the radius of the tube, physical properties of the considered fluids are constant and viscous dissipation is negligible.

Let us introduce the following transformation

$$r' = ar, \quad u' = \left[\frac{\nu}{a}\right]u, \quad v' = \left[\frac{\nu}{a}\right]v, \quad w' = \left[\frac{\nu}{a}\left(\frac{L}{2a}\right)^{1/2}\right]W, \tag{1}$$

$$T_w - T = [4aRePrG^T]H, \quad u = \frac{1}{r}\frac{\partial \Psi}{\partial \varphi}, \quad v = -\frac{\partial \Psi}{\partial r} \tag{2}$$

where ν is the kinematic viscosity,

$$G^T = -\frac{1}{L}\frac{\partial T}{\partial \theta} = \text{const.},$$

T_w the wall temperature and Pr the Prandtl number. After applying the assumptions stated above, the governing equations for the present problem in dimensionless form are

Equation for the primary flow

$$\frac{1}{r}\left(\frac{\partial \Psi}{\partial \varphi}\frac{\partial w}{\partial r} - \frac{\partial \Psi}{\partial r}\frac{\partial w}{\partial \varphi}\right) = D + \nabla^2 w. \tag{3}$$

Equation for the secondary flow

$$\frac{1}{r}\left(\frac{\partial \Psi}{\partial \varphi}\frac{\partial \zeta}{\partial r} - \frac{\partial \Psi}{\partial r}\frac{\partial \zeta}{\partial \varphi}\right) + w\frac{\partial w}{\partial r}\sin\varphi + \frac{w}{r}\frac{\partial w}{\partial \varphi}\cos\varphi = \nabla^2 \zeta \tag{4}$$

where

$$\zeta = -\nabla^2\Psi \tag{5}$$

$$\nabla^2 \equiv \frac{\partial^2}{\partial r^2} + \frac{1}{r}\frac{\partial w}{\partial r} + \frac{1}{r^2}\frac{\partial^2}{\partial \varphi^2}.$$

Energy equation

$$\frac{Pr}{r}\left(\frac{\partial \Psi}{\partial \varphi}\frac{\partial H}{\partial r} - \frac{\partial \Psi}{\partial r}\frac{\partial H}{\partial \varphi}\right) = \nabla^2 H + \frac{w}{D}. \tag{6}$$

It is noted that the vorticity function ζ is introduced here to avoid using biharmonic function $\nabla^4\Psi$ in the equation for secondary flow. The Navier–Stokes equations (3)–(5) and the energy equation (6) are nonlinear partial differential equations of elliptic type. The boundary conditions are:

$$\Psi = \frac{\partial \Psi}{\partial r} = w = T - T_w = 0 \quad \text{at } r = 1. \tag{7}$$

Because of the symmetry we have

$$\begin{aligned} \Psi(r, -\varphi) &= -\Psi(r, \varphi) \\ \zeta(r, -\varphi) &= -\zeta(r, \varphi) \\ w(r, -\varphi) &= -w(r, \varphi) \end{aligned} \tag{8}$$

and it is only necessary to consider the upper half of the circular region. Consequently, the boundary conditions are:

$$\Psi = \frac{\partial \Psi}{\partial r} = w = T - T_w = 0$$

$$\text{at } r = 1 \quad \text{and } 0 \le \varphi \le \pi, \tag{7'}$$

$$\Psi = \zeta = \frac{\partial w}{\partial \varphi} = \frac{\partial H}{\partial \varphi} = 0 \quad \text{at } \varphi = 0 \quad \text{or } \varphi = \pi \tag{8'}$$

$$\frac{\partial w}{\partial r} = 0 \quad \text{at } \varphi = \frac{\pi}{2} \quad \text{and } r = 0. \tag{8''}$$

In contrast to the forced convection problem with buoyancy effect, for the problem at hand, the momentum equations and energy equation are uncoupled and the flow problem can be solved independently.

3. FINITE DIFFERENCE APPROXIMATION AND COMPUTATIONAL PROCEDURE

We suppose the semi-circular region to be divided into a grid formed by a set of radial lines which cut a set of semicircular arcs concentric with the boundary $r = 1$ (Fig. 2). The grid points are uniformly spaced with spacing h in direction r and l in the angle φ. Let $h = [1/(M-1)]$ and $l = [\pi/(N-1)]$, where M and N are the numbers of the points in r and φ directions, respectively. In order to solve the problem (3)–(8″) we shall add the time derivatives of the functions W, ζ and H to equations (3), (4) and (6) which physically correspond to the unsteady-state problem:

$$\frac{\partial w}{\partial t} = -\frac{1}{r}\left(\frac{\partial \Psi}{\partial \varphi}\frac{\partial w}{\partial r} - \frac{\partial \Psi}{\partial r}\frac{\partial w}{\partial \varphi}\right) + D + \nabla^2 w, \tag{9}$$

$$\frac{\partial \zeta}{\partial t} = -\frac{1}{r}\left(\frac{\partial \Psi}{\partial \varphi}\frac{\partial \zeta}{\partial r} - \frac{\partial \Psi}{\partial r}\frac{\partial \zeta}{\partial \varphi}\right) + w\frac{\partial w}{\partial r} \times \sin\varphi + \frac{w}{r}\frac{\partial w}{\partial \varphi}\cos\varphi + \nabla^2\zeta, \tag{10}$$

$$\frac{\partial H}{\partial t} = -\frac{Pr}{r}\left(\frac{\partial \Psi}{\partial \varphi}\frac{\partial H}{\partial r} - \frac{\partial \Psi}{\partial \varphi}\frac{\partial H}{\partial \varphi}\right) + \nabla^2 H + \frac{w}{D}. \tag{11}$$

Since the boundary conditions (7′)–(8″) do not depend on the time, the unsteady-state problem will converge to the steady-state problem. So in our numerical solution we can apply a converge iteration technique using the time step as a parameter [13]. For the purpose of computation we use an implicit scheme that can be factored [14] into a multi-stage process with fictitious time t_1

$$\frac{\partial \Psi}{\partial t_1} = \nabla^2\Psi + \zeta. \tag{12}$$

Some difficulties arise because there are no physical boundary conditions for the vorticity ζ at the wall of the tube. That is why we have solved the equation inside the circle Ω_1 (Fig. 2). At Ω_1 we put the condition

$$\zeta^{(n+1)} = -\Delta\Psi^{(n)}$$

where n is the number of the time stage. From the condition

$$\Psi = \frac{\partial \Psi}{\partial r} = 0 \quad \text{at } \Omega$$

we find

$$\Psi/\Omega_2 = 4\Psi/\Omega_1 \quad \Psi/\Omega = 0.$$

The corresponding difference equations and boundary conditions for the flow problem are

$$\frac{\tilde{w}_{i,j}^{(p)} - w_{i,j}^{(n)}}{0.5\tau} = \left(\Lambda_r - \frac{1}{r_i}\Delta_r\tilde{\Psi}_{i,j}^{(p)}\Delta\varphi\right)\tilde{w}_{i,j}^{(p)} + \left(\Lambda\varphi + \frac{1}{r_i}\Delta\varphi\tilde{\Psi}_{i,j}^{(p)}\Delta_r\right)w_{i,j}^{(p)} + D \tag{13a}$$

for $j = 2, \ldots, N-1, \quad i = 2, \ldots, M-1, \quad w_{M,j}^{(p)} = 0,$

$$-3w_1^{(p)\frac{1+N}{2}} + 4w_2^{(p)\frac{1+N}{2}} - w_3^{(p)\frac{1+N}{2}} = 0.$$

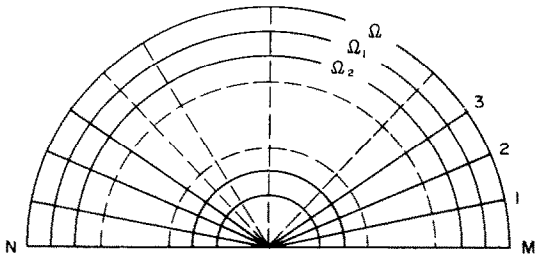

FIG. 2. Numerical grid in the tube cross section.

$$\frac{\tilde{w}_{i,j}^{(p)} - \bar{w}_{i,j}^{(p)}}{0.5\tau} = \left(\Lambda_r - \frac{1}{r_i}\Delta_r \tilde{\Psi}_{i,j}^{(p)} \Delta\varphi\right)\bar{w}_{i,j}^{(p)} + \left(\Lambda\varphi + \frac{1}{r_i}\Delta\varphi\,\tilde{\Psi}_{i,j}^{(p)}\Delta_r\right)\tilde{w}_{i,j}^{(p)} + D \quad (13^{\delta})$$

for $i = 2,\ldots,M-1$, $j = 2,\ldots,N-1$, $\tilde{w}_{i,N}^{(p)} = \tilde{w}_{i,N-1}^{(p)}$, $\tilde{w}_{i,1}^{(p)} = \tilde{w}_{i,2}^{(p)}$,

$$\frac{\bar{\zeta}_{i,j}^{(p)} - \zeta_{i,j}^{(n)}}{0.5\tau} = \left(\Lambda_r - \frac{1}{r_i}\Delta_r \tilde{\Psi}_{i,j}^{(p)} \Delta_\varphi\right)\bar{\zeta}_{i,j}^{(p)} + \left(\Lambda\varphi + \frac{1}{r_i}\Delta\varphi\,\tilde{\Psi}_{i,j}^{(p)}\Delta_r\right)\zeta_{i,j}^{(n)} + F_{i,j} \quad (14^{a})$$

for $i = 2,\ldots,M-2$, $j = 2,3,\ldots,N-1$, $\bar{\zeta}_{M-1,j}^{(p)} = -(\Lambda_r + \Lambda_\varphi)\Psi_{M-1,j}^{(p)}$,

$$\frac{\tilde{\zeta}_{i,j}^{(p)} - \bar{\zeta}_{i,j}^{(p)}}{0.5\tau} = \left(\Lambda_r - \frac{1}{r_i}\Delta_r \tilde{\Psi}_{i,j}^{(p)} \Delta\varphi\right)\bar{\zeta}_{i,j}^{(p)} + \left(\Lambda\varphi + \frac{1}{r_i}\Delta\varphi\,\tilde{\Psi}_{i,j}^{(p)}\Delta_r\right)\zeta_{i,j}^{(n+1)} + F_{i,j} \quad (14^{b})$$

for $\tilde{\zeta}_1^{(p)} = 0, \tilde{\zeta}_{i,N}^{(p)} = 0, j = 2,\ldots,N-1, i = 2,\ldots,M-2$;

$$\frac{\bar{\Psi}_{i,j}^{(p)} - \tilde{\Psi}_{i,j}^{(p)}}{\tau_1} = \Lambda_r \bar{\Psi}_{i,j}^{(p)} + \tilde{\zeta}_{i,j}^{(p)} \quad (15^{a})$$

for $i = 2, M = 2, j = 2,\ldots,N-1, \Psi_{i,j} = 0, \Psi_{M-2,j} = 4\varphi_{M-1,j}$, $\varphi_{M,j} = 0$,

$$\frac{\tilde{\Psi}^{(p+1)} - \bar{\Psi}^{(p)}}{\tau_1} = \Lambda\varphi\,\tilde{\Psi}^{(p+1)} \quad (15^{\delta})$$

for $i = 2,\ldots,M-2, j = 2,\ldots,N-2, \Psi_{i,1} = \Psi_{i,N} = 0$. Here

$$\Lambda_r\Phi_{ij} = \frac{\left(1 + \frac{h}{2r_i}\right)\Phi_{i+1,j} - 2\Phi_{ij} + \left(1 + \frac{h}{2r_i}\right)\Phi_{i-1,j}}{h^2},$$

$$\Lambda_\varphi\Phi_{ij} = \frac{\Phi_{i,j+1} - 2\Phi_{i,j} + \Phi_{i,j-1}}{r_i^2 l^2},$$

$$\Delta_\varphi\Phi_{ij} = \frac{\Phi_{i,j+1} - \Phi_{i,j-1}}{2l},$$

$$\Delta_r\Phi_{ij} = \frac{\Phi_{i+1,j} - \Phi_{i,j-1}}{2h},$$

$$F_{ij} = w_{ij}\left(\Delta_r w_{ij}\sin\varphi_j + \frac{1}{r_i}\Delta\varphi w_{i,j}\cos\varphi_j\right).$$

The iterative procedure begins with solving the equations (13) and (14). We put $\tilde{\Psi}^{(1)} = \Psi^{(n)}$ and do an entire spacing in respect to the physical time, where $\Psi^{(n)}$ is taken from the previous stage. After obtaining $\tilde{\zeta}^{(1)}$ we do a spacing in respect to fictitious time t_l in equations (15) and get $\tilde{\Psi}^{(2)}$. By means of $\Psi^{(2)}$ we repeat the procedure to find $\tilde{\zeta}^{(2)}$ and $\tilde{w}^{(2)}$. Iteration is terminated when the following relative error criterion is satisfied:

$$\max_{i,j}\left|\frac{\Psi_{i,j}^{(p+1)} - \Psi_{i,j}^{(p)}}{\Psi_{i,j}^{(p)}}\right| < 0.0001.$$

Then we take

$$w^{(n+1)} = \tilde{w}^{(p+1)} \quad \zeta^{(n+1)} = \tilde{\zeta}^{(p+1)} \quad \Psi^{(n+1)} = \tilde{\Psi}^{(p+1)}$$

and obtain the values of the computed functions W, ζ and Ψ over the new time stage.

The physical time iteration is terminated when the following criterion is satisfied

$$\max_{i,j}\left\{\left|\frac{\zeta_{i,j}^{(n+1)} - \zeta_{i,j}^{(n)}}{\zeta_{i,j}^{(n+1)}}\right|, \left|\frac{w_{i,j}^{(n+1)} - w_{i,j}^{(n)}}{w_{i,j}^{(n+1)}}\right|\right\} \le 0.0001.$$

Because of the inner iteration about the iteration parameter t_l actually according to physical time t, one solves the following problem

$$\frac{w^{(n+1/2)} - w^{(n)}}{0.5\tau} = \left(\Lambda_r - \frac{1}{r_i}\Delta\varphi\Psi^{(n+1)}\Delta_r\right)w^{(n+1/2)} + \left(\Lambda\varphi + \frac{1}{r_i}\Delta_r\Psi^{(n+1)}\Delta\varphi\right)w^{(n)} + D,$$

$$\frac{w^{(n+1)} - w^{(n+1/2)}}{0.5\tau} = \left(\Lambda_r - \frac{1}{r_i}\Delta\varphi\Psi^{(n+1)}\Delta_r\right)w^{(n+1/2)} + \left(\Lambda\varphi + \frac{1}{r_i}\Delta_r\Psi^{(n+1)}\Delta_r\right)w^{(n+1)} + D.$$

This scheme is non-linear implicit and therefore absolutely stable. It is worth noting that the finite-difference equations (13)–(15) are for order $O(\tau + \tau_1 + h^2)$ with exception to the points along $\varphi = 0$ and $\varphi = \pi$, where the order of the numerical scheme is $O(\tau + \tau_1 + h)$.

The finite difference approximation of the energy equation (11) has the form

$$\frac{\bar{H}_{i,j}^{(n)} - H_{i,j}^{(n)}}{0.5\tau} = -\frac{Pr}{r}(\Delta\varphi\Psi_{ij}\Delta_r H_{ij}^{(n+1)} - \Delta_r\Psi_{ij}\Delta\varphi\bar{H}_{ij}^{(n)}) + \Lambda_r H_{ij}^{(n+1)} + \Lambda\varphi\bar{H}_{ij}^{(n)} + \frac{w_{i,j}}{D},$$

$$\frac{H_{i,j}^{(n+1)} - \bar{H}_{i,j}^{(n)}}{0.5\tau} = -\frac{Pr}{r}(\Delta\varphi\Psi_{ij}\Delta_r H_{ij}^{(n+1)} - \Delta_r\Psi_{ij}\Delta\varphi\bar{H}_{ij}^{(n)}) + \Lambda_r H_{ij}^{(n+1)} + \Lambda\varphi H_{ij}^{(n)} + \frac{w_{i,j}}{D}.$$

The boundary conditions are:

at $r = 1$, $H_{M,j} = 0$, $j = 1,2,\ldots,N$.

at $\varphi = 0$

$$\bar{H}_{i,1}^{(n)} = \frac{\tau}{r_i^2 l^2 + r}\bar{H}_{i,2}^{(n)} + \frac{r_i^2 l^2 \tau}{2(r_i^2 l^2 + \tau)} \times\left[\Lambda_r H_{i,1}^{(n)} - \frac{Pr\Psi_{i,2}}{2r_i l}H_{i,1}^{(n)} + \frac{H_{i,1}^{(n)}}{0.5\tau} + \frac{w_{i,1}}{D}\right],$$

at $\varphi = \pi$

$$\bar{H}^{(n)}_{i,N-1} = \frac{r_i^2 l^2 + \tau}{\tau}\bar{H}^{(n)}_{i,N} - \frac{r_i^2 l^2}{2} \times \left[\Lambda_r H^{(n)}_{i,N} + \frac{Pr\Psi_{i,N-1}}{2r_i l}\Delta_r H^{(n)}_{i,N} + \frac{H_{i,N}}{0.5} - \frac{w_{i,N}}{D}\right].$$

4. FLOW AND HEAT TRANSFER RESULTS

When a fluid flows through a curved tube, a pressure gradient directed towards the centre of curvature is set up across the tube to balance the centrifugal force arising from the curvature. The fluid in the middle of the pipe moves outwards and that above and below it moves inwards. Thus in the tube the secondary flow has the effect of shifting the high velocity region towards the outer wall and creating a much thicker layer of slowly moving fluid at the inner wall. The resultant combined primary and secondary flow causes a fluid element to have a screw-like motion. The low-Dean secondary flow stream lines are essentially symmetrical and convex [1, 2]. As a Dean number is increased, causing an intensification of the secondary flow, non-convex regions are developed by the formation of dimples in the streamlines of the secondary flow in the plane of the cross-section and the lines of constant axial velocity W are given in Figs. 3–5 for Dean numbers equal to 2000, 5000, 7000 respectively. It is not surprising that there is a movement at the axial velocity peak nearer to the outer wall. The centrifugal force which drives the secondary flow itself takes much greater values on the outside of the bend. The form of the streamlines shows that the secondary flow components take much greater values on the inside of the tube. The curves of constant W show the tendency of a central core region to develop as D increases. Within this region there is a sub-region which is far from the walls of the tube and where viscous forces are small.

In Figs. 6–8 the constant dimensionless values of temperature H is shown for different Dean and Prandtl numbers. For low Prandtl number the maximum

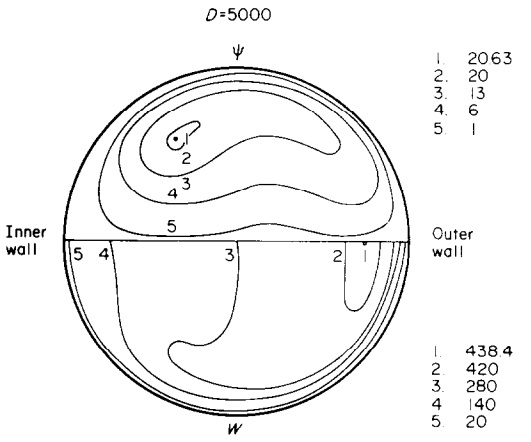

FIG. 4. Streamlines for secondary flow and isolines for axial velocity at $D = 5000$.

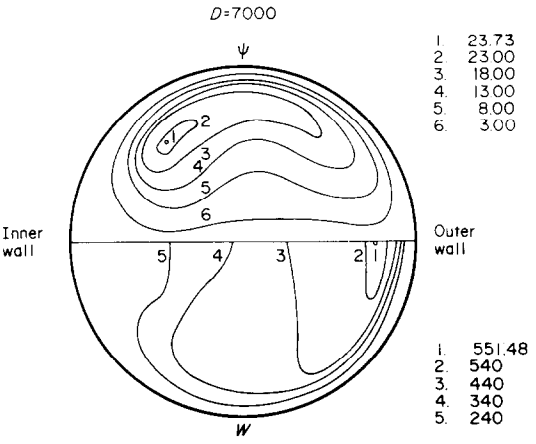

FIG. 5. Streamlines for secondary flow and isolines for axial velocity at $D = 7000$.

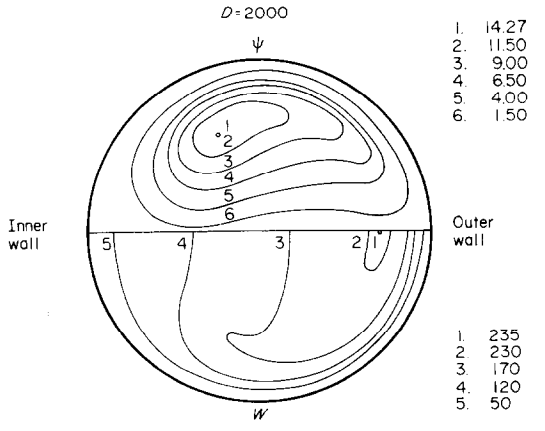

FIG. 3. Streamlines for secondary flow and isolines for axial velocity at $D = 2000$.

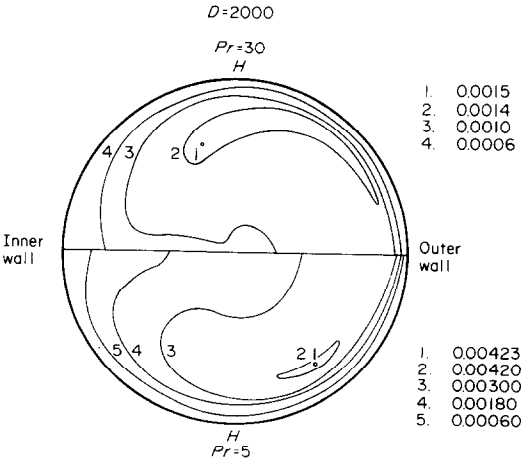

FIG. 6. Isothermals for $D = 2000$ at $Pr = 30$ and $Pr = 5$ respectively.

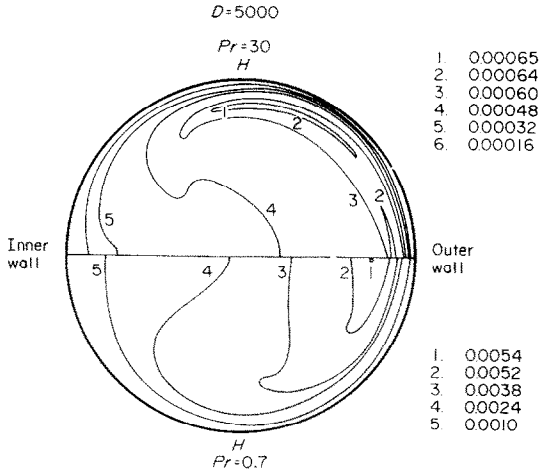

FIG. 7. Isothermals for $D = 5000$ at $Pr = 30$ and $Pr = 0.7$ respectively.

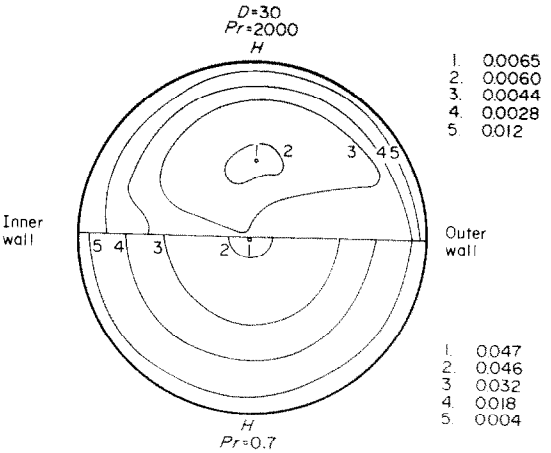

FIG. 8. Isothermals for $D = 30$ at $Pr = 2000$ and $Pr = 0.7$ respectively.

temperature occurs at points near the diameter of symmetry. The temperature profiles for Prandtl number of 0.7 (Figs. 6 and 7) are skewed toward the outer wall. A typical contour of dimensionless temperature for higher Prandtl number is given in Fig. 8, where $Pr = 2000$.

One can see, from equation (6), that as the Dean number increases, the effect of the convective terms also increases for a given Prandtl number. As the Prandtl number increases, the effect of the convective terms also increases for a given Dean number. So the effect of the Dean number is equivalent to the effect of the Prandtl number. The heat transfer results from the present analysis is compared with the result from Kalb and Seader [12]. As we can see from Table 1 our calculations essentially exceed those of [12].

The local Nusselt number is defined by

$$Nu = \frac{-2\left(\frac{\partial H}{\partial r}\right)_{r=1}}{H_m}$$

where

$$H_m = \frac{1}{\pi \cdot W_m} \int_0^{\pi} \int_0^1 Hwr\,dr\,d\varphi$$

is the flow-averaged mean value of H over the flow cross section and

$$W_m = \frac{1}{\pi} \int_0^{\pi} \int_0^1 wr\,dr\,d\varphi$$

is the mean of W over the cross section of the tube.

Therefore, the peripheral averaged Nusselt number Nu equals to

$$\bar{Nu} = \frac{-2\int_0^{\pi}\left(\frac{\partial H}{\partial r}\right)_{r=1} d\varphi \cdot \int_0^{\pi}\int_0^1 wr\,dr\,d\varphi}{\pi \int_0^{\pi}\int_0^1 Hwr\,du\,d\varphi}.$$

The average Nusselt number is plotted for low Dean numbers and high Prandtl numbers in Fig. 9. One can see that the average Nusselt number increases with the increase of the Prandtl number even when the Dean number is held constant. Figure 10 shows the effect of Dean number on the peripheral average Nusselt number Nu for Prandtl numbers $Pr = 0.7$ and $Pr = 5$.

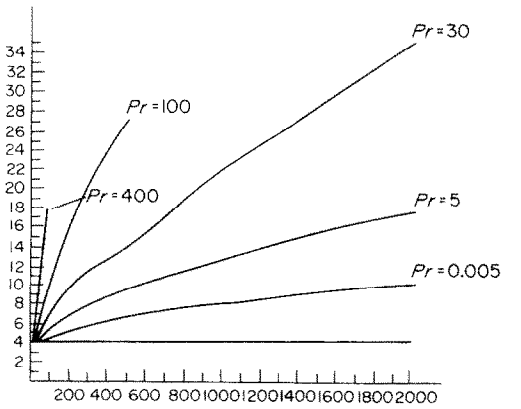

FIG. 9. Numerical results for peripherally average Nusselt number at low Dean numbers.

Table 1

	Pr	2000	1600	800	400	100	30
[12]	D	—	33.44	56.56	85.85	105.5	860.7
Present	D	43.33	43.33	60	100	500.0	5000

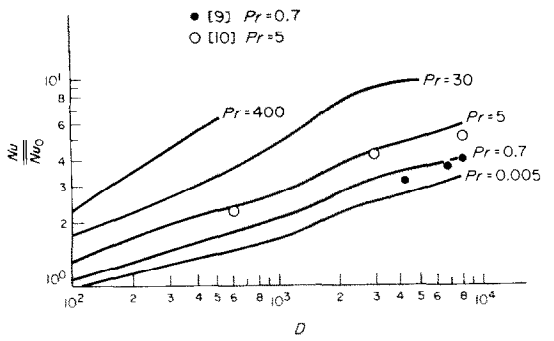

FIG. 10. Comparison of the numerical results with experimental data for high Dean numbers.

Here we give the comparison of our numerical results with experimental work [9].

5. CONCLUSIONS

The method of fractional steps has been successfully applied to hydrodynamically and thermally fully developed steady flow of viscous incompressible fluid in a curved circular tube. No numerical difficulties have been encountered. The comparisons show very good agreement of our results with available experimental data and some theoretical solutions.

Further tasks are the following:

(i) Application of the method to the non-steady fully developed flow in a curved tube;

(ii) Extension of the method to the three-dimensional developing entry steady flow, both hydrodynamic and thermal, in helically coiled tubes.

Work on these tasks is currently in progress.

REFERENCES

1. W. R. Dean, Note on the motion of fluid in curved pipe. *Phil. Mag. Ser.* 7(4), 208–223 (1927).
2. S. N. Barua, On secondary flow in stationary curved pipes. *Q. J. Mech. Appl. Math.* **16**, 61–77 (1963).
3. D. J. McConalogue and R. S. Srivastava, Motion of a fluid in a curved tube, *Proc. R. Soc.* **A307**, 37–53 (1968).
4. L. C. Truesdell and R. J. Adler, Numerical treatment of fully developed laminar flow in helically coiled tubes, *A.I.Ch.E. J.* **16**, 1010–1015 (1970).
5. D. Greenspan, Secondary flow in a curved tube, *J. Fluid Mech.* **57**, 167–176 (1973).
6. W. M. Collins and S. C. R. Dennis, The steady motion of a viscous fluid in a curved tube, *Q. J. Mech. Appl. Math.* **28**, 133–156 (1975).
7. Z. Zapryanov and Ch. Christov, Fully developed flow of viscous incompressible fluid in toroidal tube with circular cross-section, *Theoret. Appl. Mech.* **8**, 11–17 (1977).
8. S. V. Patankar, V. S. Pratap and D. B. Spalding, Prediction of laminar flow and heat transfer in helically coiled pipes, *J. Fluid Mech.* **62**, 539–551 (1974).
9. Y. Moti and W. Nakayama, Study of forced convective heat transfer in curved pipes, *Int. J. Heat Mass Transfer* **8**, 67–82 (1965).
10. A. N. Dravid, K. A. Smith, E. W. Merrill and P. L. T. Brian, Effect of secondary fluid motion on laminar flow heat transfer in helically coiled circular pipes, *A.I.Ch.E.J.* **17**, 1114–1122 (1971).
11. L. R. Austin and J. D. Seader, Fully developed viscous flow in coiled circular pipes, *A.I.Ch.E. J.* **19**, 85–94 (1973).
12. C. E. Kalb and J. D. Seader, Heat and mass transfer phenomena for viscous flow in curved circular tubes, *Int. J. Heat Mass Transfer* **15**, 801–817 (1972).
13. J. Douglas, Jr. and H. H. Rachford, Jr., On the numerical solution of heat conduction problems in two and three space variables. *Trans. Am. Math. Soc.* **82**, 421–439 (1956).
14. N. N. Yanenko, *The Method of Fractional Steps*, McGraw-Hill (1971).

ECOULEMENT LAMINAIRE ETABLI ET TRANSFERT THERMIQUE DANS LES TUBES CINTRES

Résumé—On étend la méthode des pas fractionnels aux problèmes hydrodynamiques et thermiques pour l'écoulement permanent et établi d'un fluide visqueux incompressible dans un tube circulaire cintré. Cette méthode numérique fournit une bonne solution pour les nombres de Dean et les nombres de Prandtl faibles et raisonablement élevés. Des exemples sont donnés pour les profils de vitesse axiale et de température, pour les isothermes. Des comparaisons sont faites entre les résultats numériques, les données expérimentales et quelques solutions théoriques.

VOLL AUSGEBILDETE LAMINARSTRÖMUNG UND WÄRMEÜBERGANG IN GEKRÜMMTEN ROHREN

Zusammenfassung—Diese Arbeit befaßt sich mit der Erweiterung des Differenzenverfahrens für hydrodynamische und thermische Probleme bei der voll ausgebildeten stationären Strömung eines viskosen, inkompressiblen Fluids in einem gekrümmten, kreisrunden Rohr. Dieses numerische Verfahren führt bei kleinen und bei mäßig hohen Dean- und Prandtl-Zahlen zu guten Lösungen. Typische Beispiele für axiale Geschwindigkeits- und Temperaturprofile, für Stromlinien und für Geschwindigkeitsprofile der Sekundärströmung, sowie für die Isothermen werden wiedergegeben. Die numerisch errechneten Geschwindigkeits- und Temperaturprofile werden mit Versuchsdaten und mit einigen theoretischen Lösung verglichen.

ПОЛНОСТЬЮ РАЗВИТОЕ ЛАМИНАРНОЕ ТЕЧЕНИЕ И ТЕПЛОПЕРЕНОС В ИЗОГНУТЫХ ТРУБАХ

Аннотация — Метод дробных шагов обобщен на гидродинамические и тепловые задачи при полностью развитом стационарном течении вязкой несжимаемой жидкости в изогнутой круглой трубе. Такой численный метод дает хорошие результаты в диапазоне от малых до умеренно больших значений чисел Дина и Прандтля. Приведены типичные распределения аксиальной скорости и температуры, линии тока, а также профили скорости вторичного течения и изотермы. Дано сравнение результатов численных расчетов профилей скорости и температуры с экспериментальными данными и с рядом других теоретических решений.